Electronic Supplementary Material (ESI) for New Journal of Chemistry

ELECTRONIC SUPPORTING INFORMATION

Synthesis of spin crossover nano-objects with different morphologies and properties

Alexey Tokarev,[a] Lionel Salmon,[a*] Yannick Guari,[b] Gábor Molnár[a] and Azzedine Bousseksou[a*]

[a] *Laboratoire de Chimie de Coordination, CNRS & Université de Toulouse (UPS, INP), 31077 Toulouse, France*

[b] *Institut Charles Gerhardt Montpellier, UMR5253, Chimie Moléculaire et Organisation du Solide, Université Montpellier II, Place E. Bataillon, 34095, Montpellier cedex 5, France.*

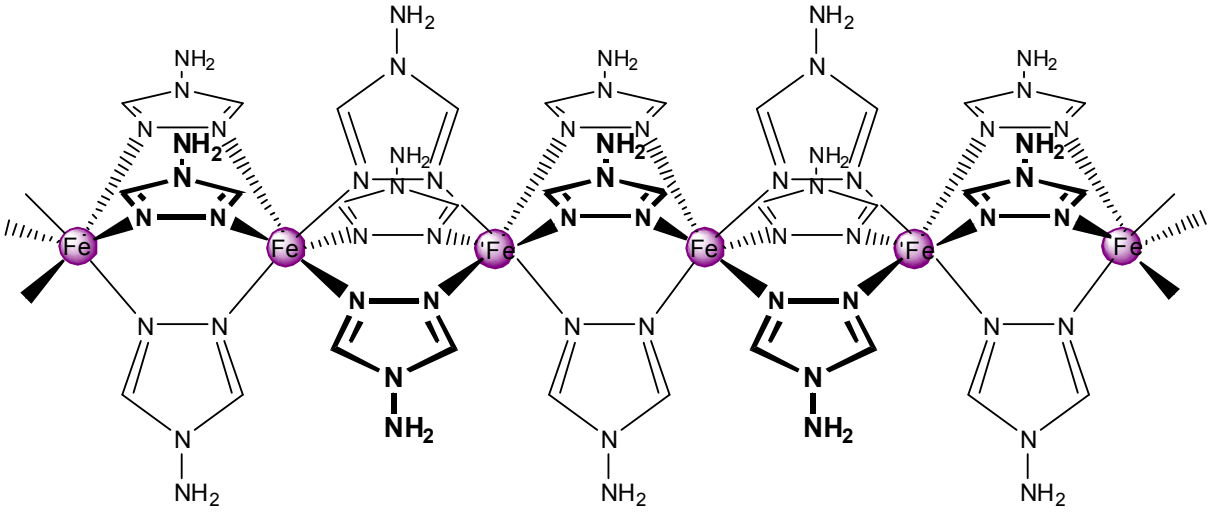

Figure S1. Schematic representation of the polymeric spin crossover $[Fe(NH_2\text{-trz})_3^{2+}]_n$ complex.

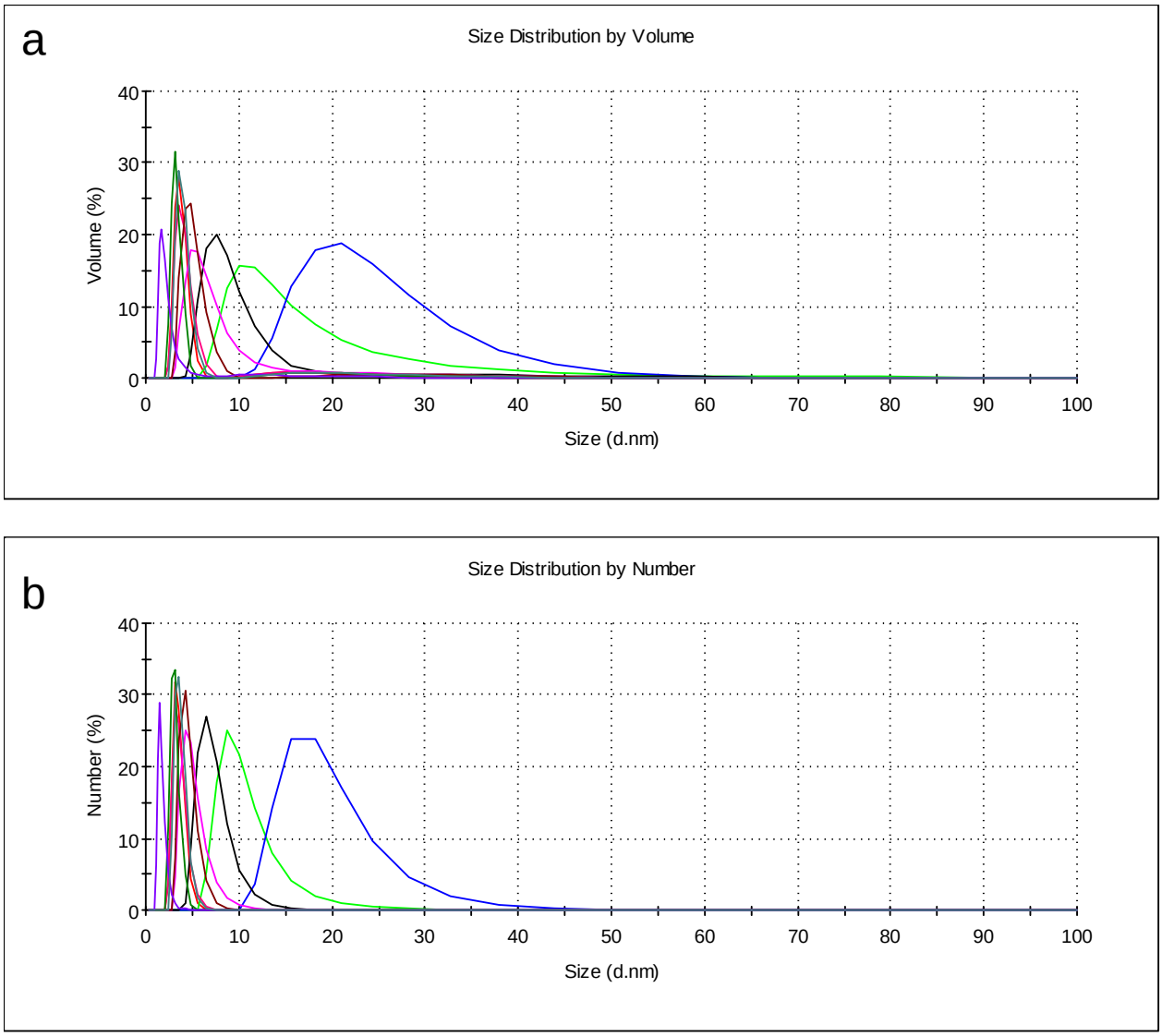

Figure S2. Volume- (a) and number-based (b) particle size distribution for the colloidal suspension **1a** at 293 K obtained by DLS analysis. (Parameters used for the data analysis: viscosity = 43 cP, refractive index = 1.450).

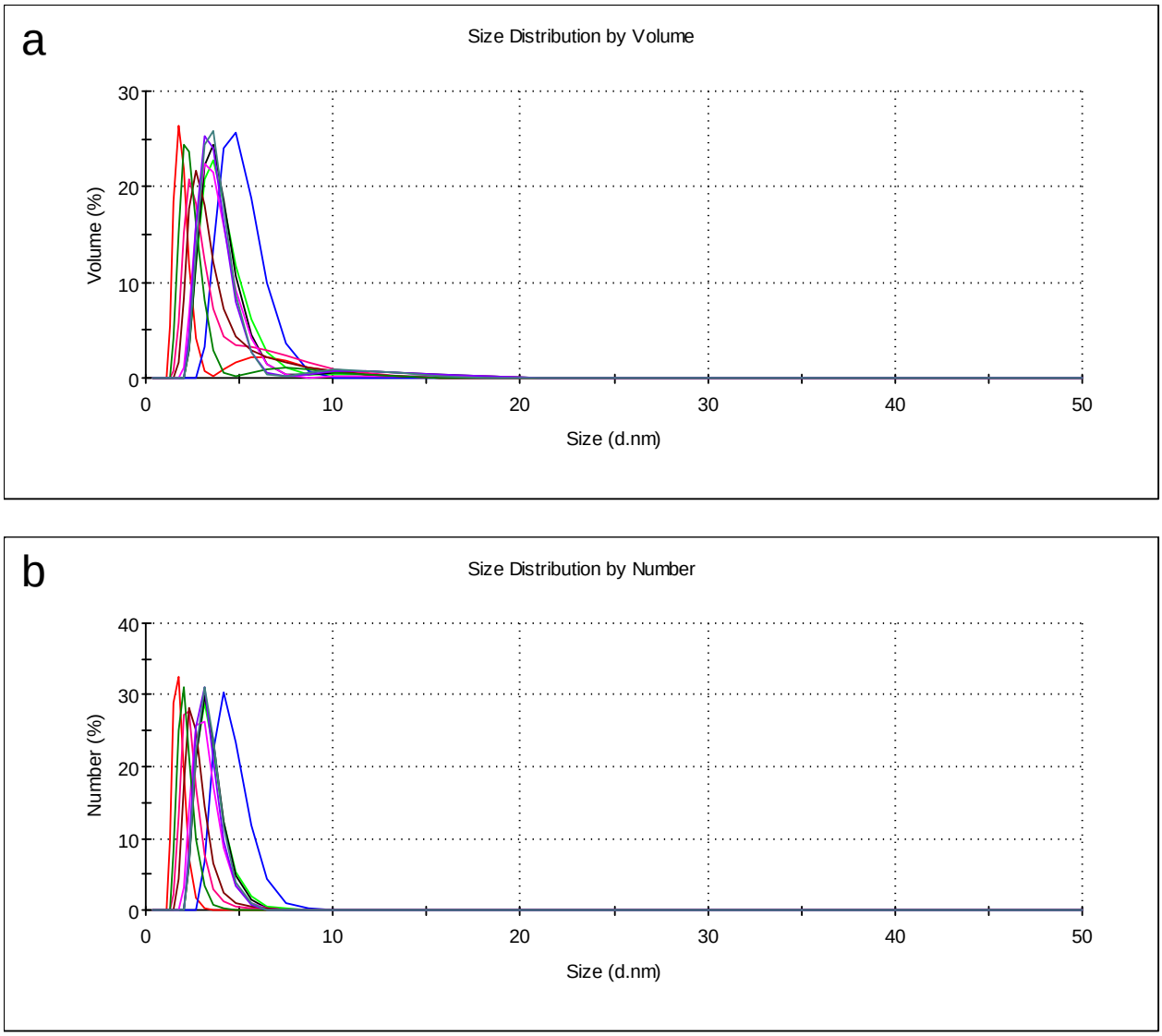

Figure S3. Volume- (a) and number-based (b) particle size distribution for the colloidal suspension **2a** at 293 K obtained by DLS analysis. (Parameters used for the data analysis: viscosity = 47 cP, refractive index = 1.450).

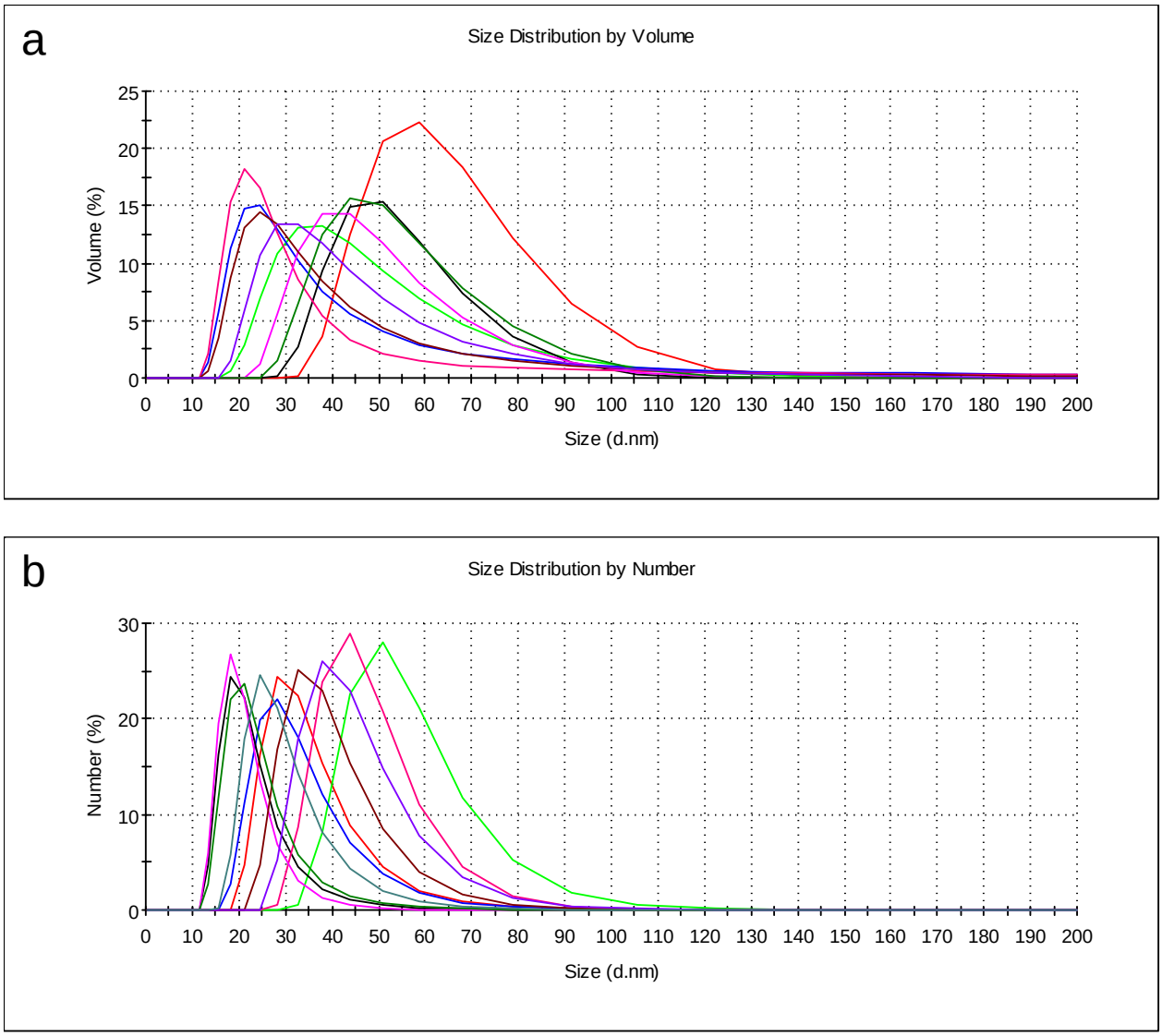

Figure S4. Volume- (a) and number-based (b) particle size distribution for the colloidal suspension **3a** at 293 K obtained by DLS analysis. (Parameters used for the data analysis: viscosity = 50 cP, refractive index = 1.450).

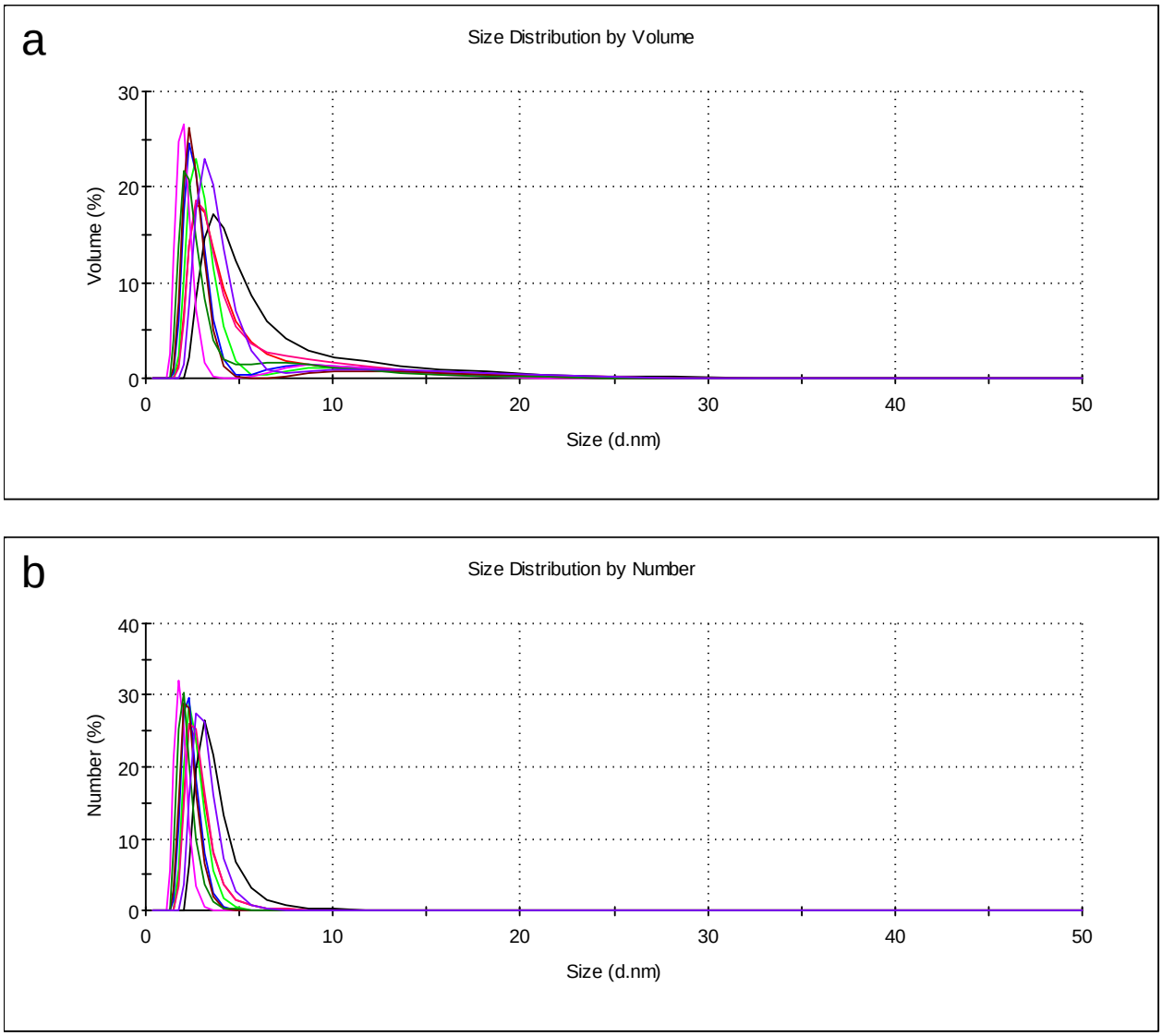

Figure S5. Volume- (a) and number-based (b) particle size distribution for the colloidal suspension **4a** at 293 K obtained by DLS analysis. (Parameters used for the data analysis: viscosity = 60 cP, refractive index = 1.450).

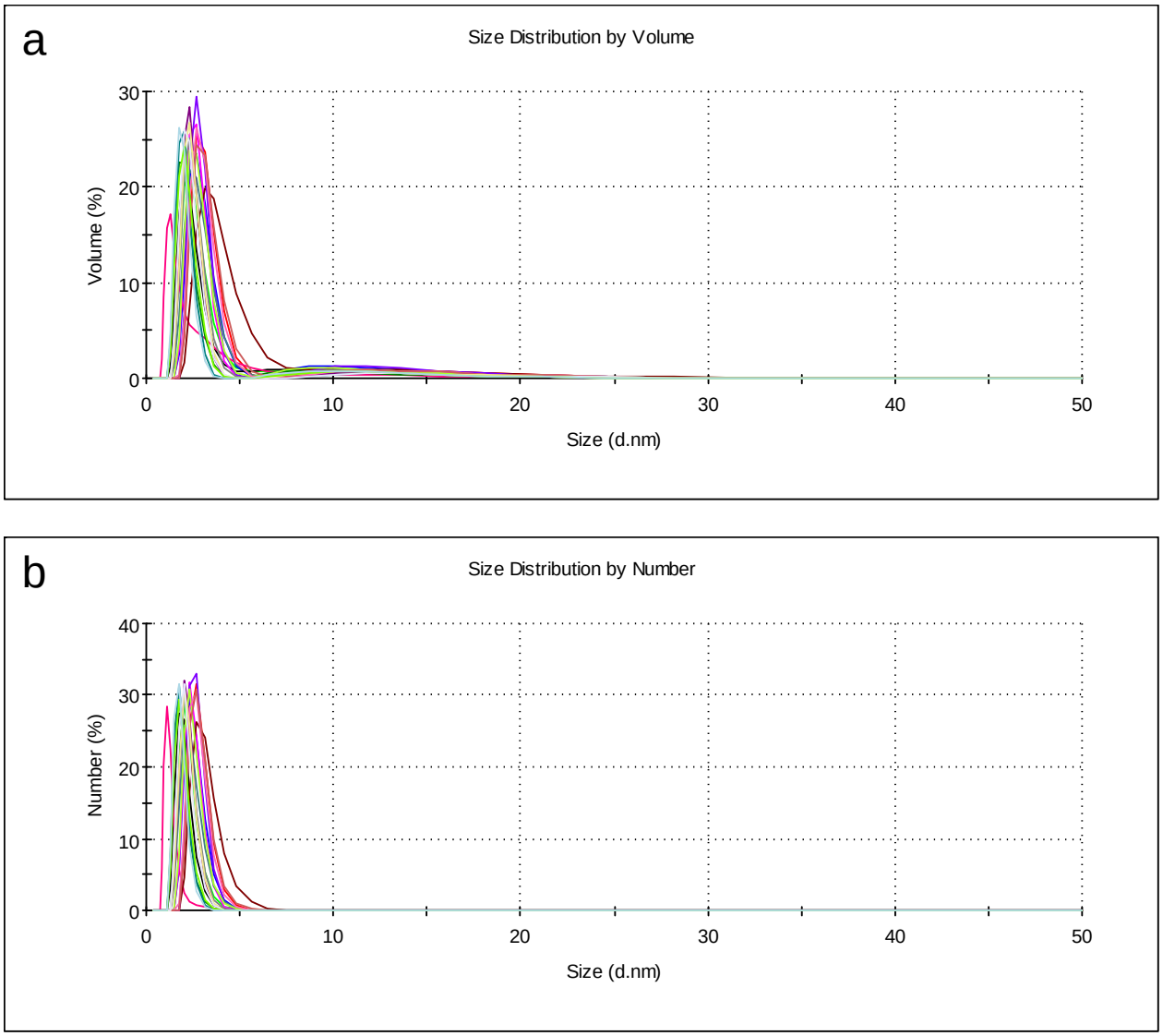

Figure S6. Volume- (a) and number-based (b) particle size distribution for the colloidal suspension **4a** isothermally held and measured by DLS analysis at 313 K. (Parameters used for the data analysis: viscosity = 21 cP, refractive index = 1.450).

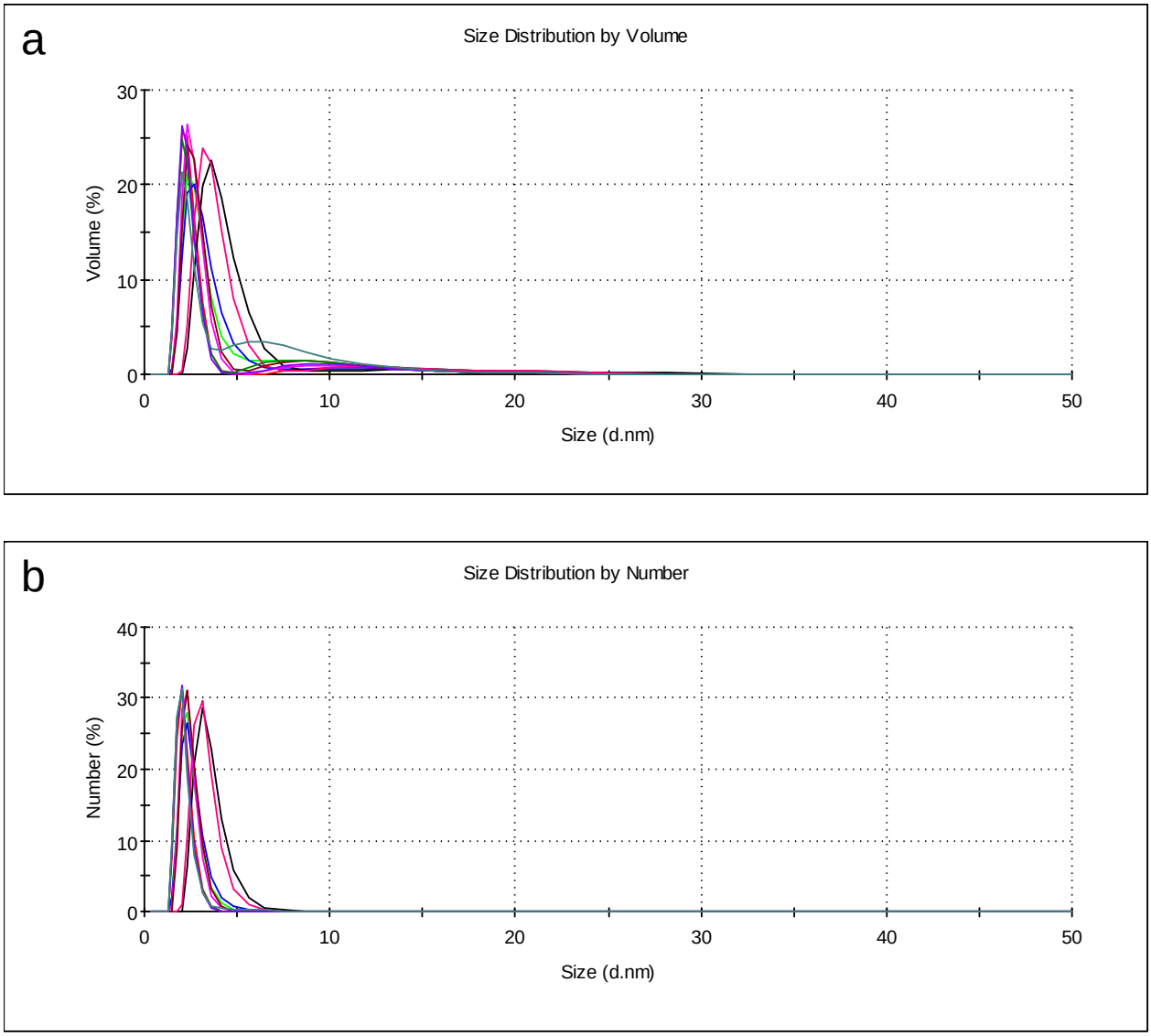

Figure S7. Volume- (a) and number-based (b) particle size distribution for the colloidal suspension **4a** measured by DLS analysis at 293 K after holding at 313 K. (Parameters used for the data analysis: viscosity = 60 cP, refractive index = 1.450).

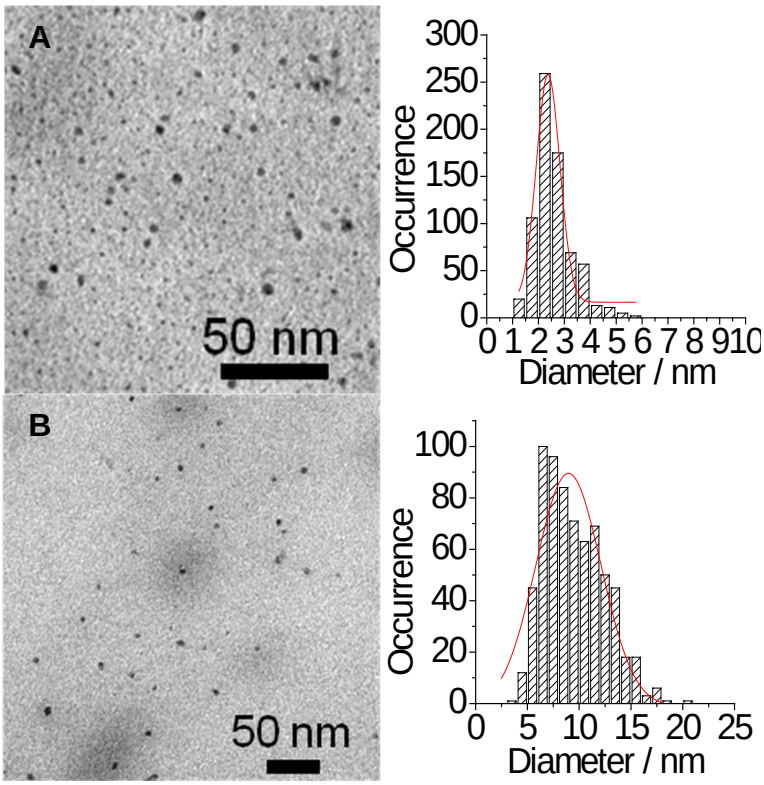

Figure S8. Cryo-mycrotomy TEM images and the size distributions for **5a** (A) and **6a** (B).

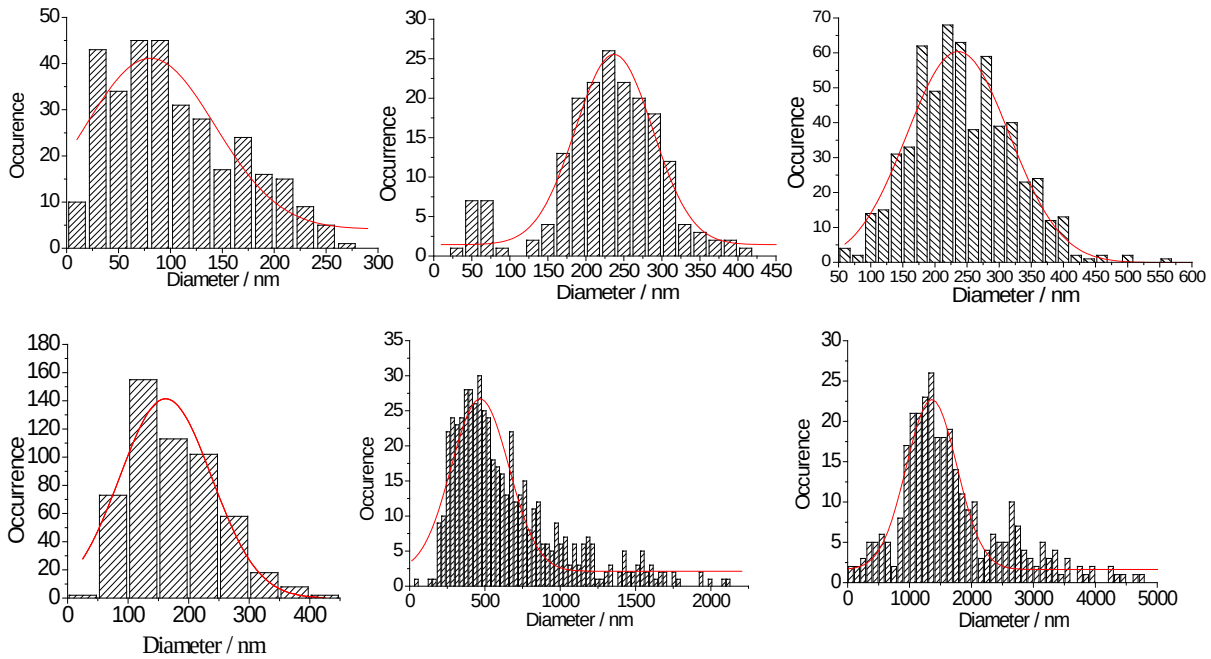

Figure S9. Size distribution of the solid state nanoparticle samples obtained by TEM: top row - **1b** (left), **2b** (middle) and **3b** (right), bottom row - **4b** (left), **5b** (middle) and **6b** (right)

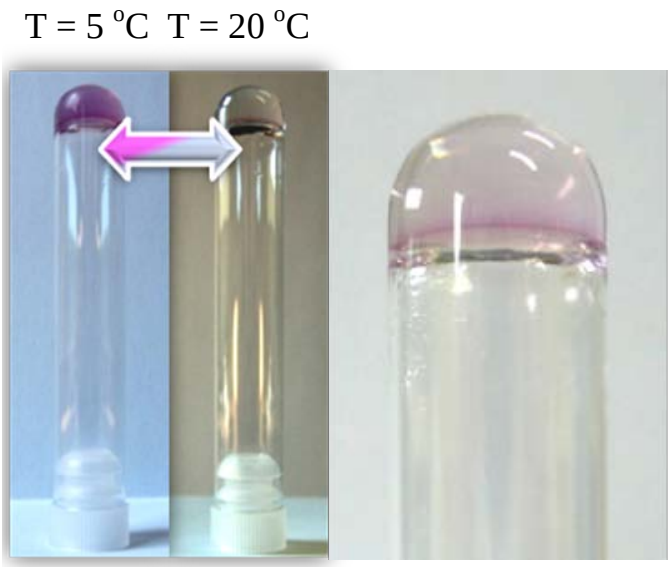

Figure S10. Photographs of the gel obtained from sample **4a**.

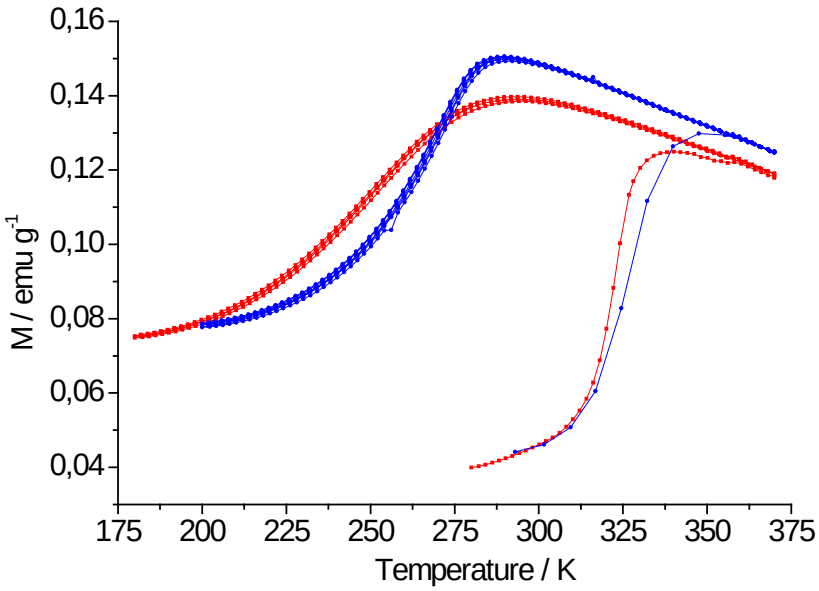

Figure S11. Temperature dependence of the magnetization for the surfactant-free fibres (red) and the solid state nanoparticles **4b** (blue) recorded in the cooling and heating modes at 1 K min^{-1} following a first heating to 370 K (dehydration). Both compounds were obtained from the microemulsion **4**.

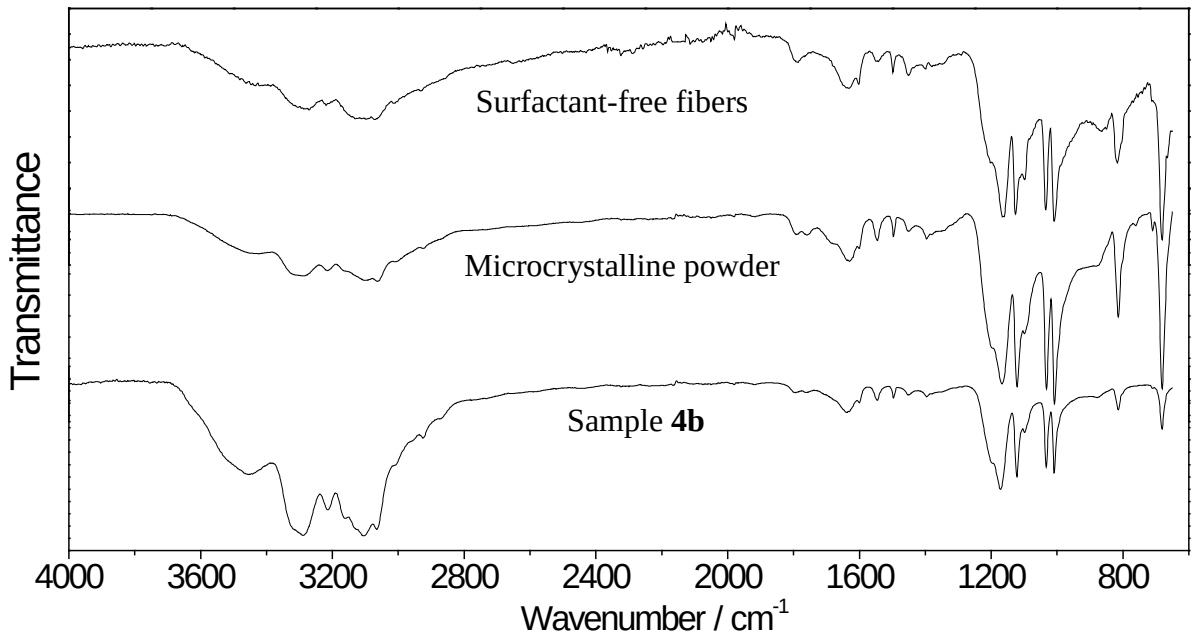

Figure S12. IR spectra of the surfactant-free fibers (top), microcrystalline powder (middle) and the nanoparticles of **4b** (bottom).

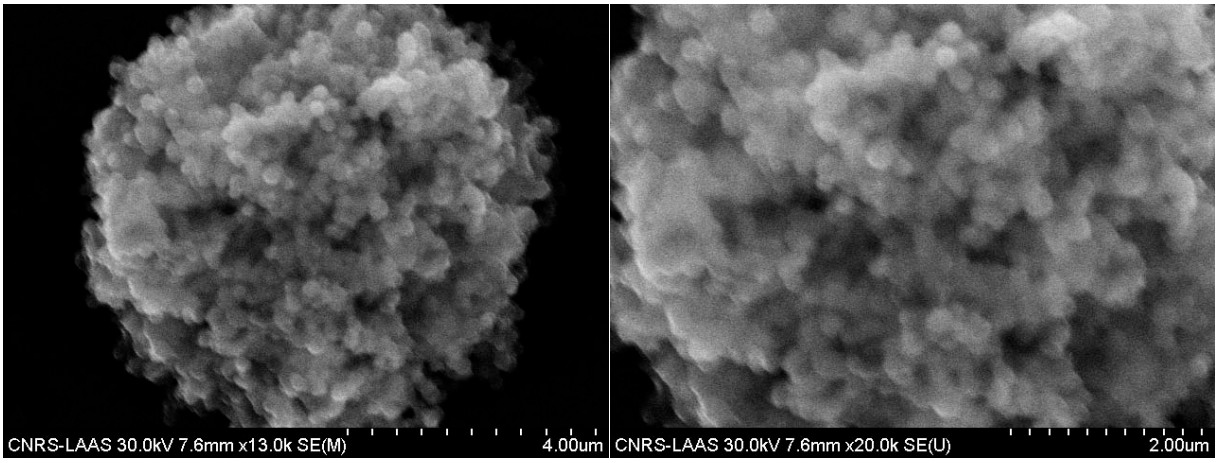

Figure S13. SEM images of sample **1b**

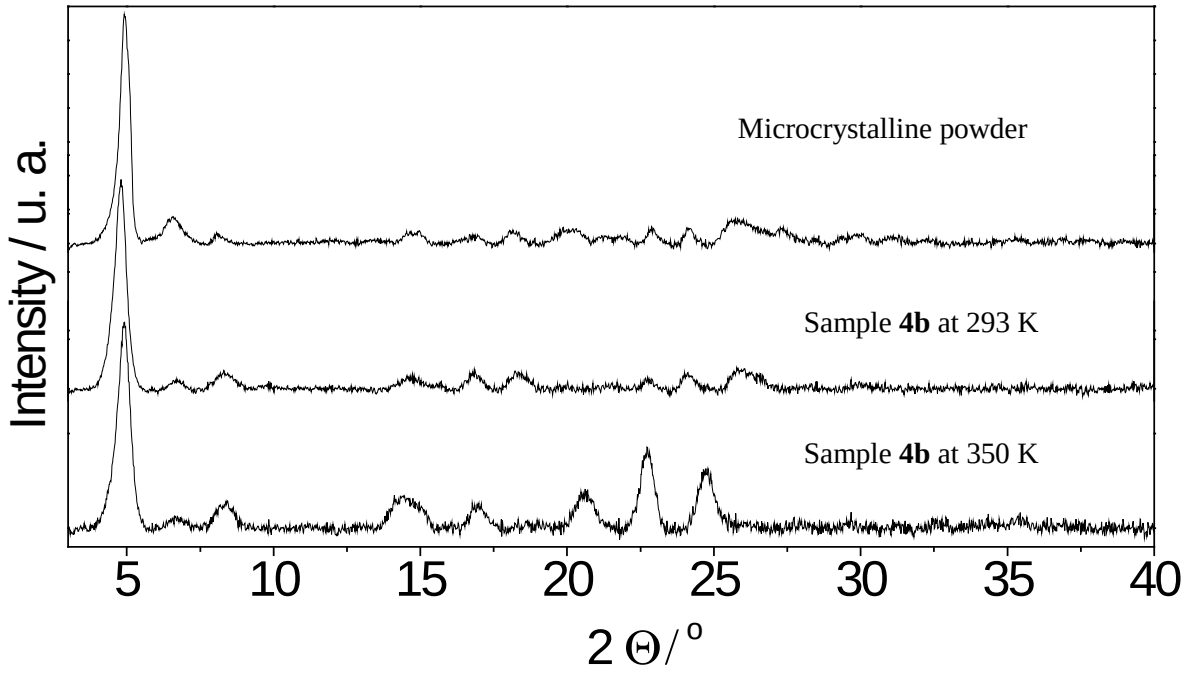

Figure S14. X-ray powder diffraction patterns for the microcrystalline powder at 293 K (top), sample **4b** at 293 K (middle) and sample **4b** at 350 K (bottom).

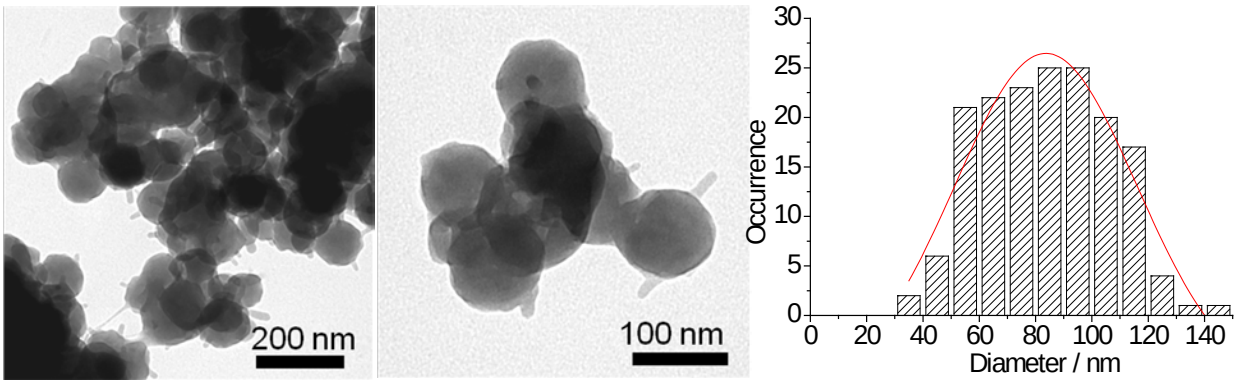

Figure S15. TEM images of $[Fe(Htrz)_2(trz)](BF_4)$ nanoparticles and their size distribution

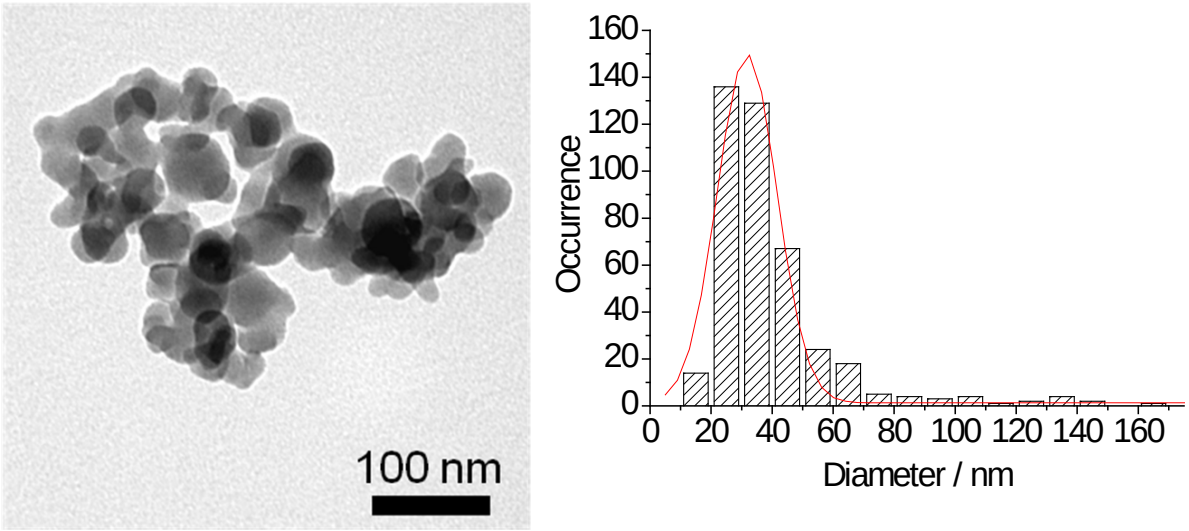

Figure S16. TEM image of $[Fe(NH_2trz)_3]Cl_2$ nanoparticles and their size distribution